Ore Geology Reviews

Metal source of giant Huize Zn-Pb deposit in SW China: New constraints from *in situ* Pb isotopic compositions of galena

Zhiwei Bao[a,*], Qun Li[a,b], Christina Yan Wang[a]

[a] *Key Laboratory for Mineralogy and Metallogeny, Guangzhou Institute of Geochemistry, Chinese Academy of Sciences, Guangzhou 5106410, China*
[b] *University of Chinese Academy of Sciences, Beijing 100049, China*

ABSTRACT

The Huize Zn-Pb deposit in SW China is a large Mississippi Valley-type (MVT) deposit containing more than 7 Mt Pb and Zn reserves at an ore grade of ~25–35% Pb + Zn, and it also contains economically important resources of Ag, Cd, In, Ge and Ga. To provide better constraints on the major source of the ore metals in the deposit *in situ* Pb isotope composition analyses were carried out by using femtosecond laser-ablation multi-collector inductively coupled plasma mass spectrometry (fs-LA-MC-ICP-MS). The results indicate that the galena grains overall have restricted Pb isotopic compositions with $^{206}Pb/^{204}Pb$ of 18.486–18.526, $^{207}Pb/^{204}Pb$ of 15.738–15.806, and $^{208}Pb/^{204}Pb$ of 38.914–39.076, which are distinctively different from those for the host dolostones and Permian Emeishan flood basalts. However, the clastic sequence composed of sandstone, siltstone and slate of Proterozoic Kunyang Group has $^{206}Pb/^{204}Pb$ of 18.789–23.274, $^{207}Pb/^{204}Pb$ of 15.712–16.005, and $^{208}Pb/^{204}Pb$ of 38.169–38.933, slightly radiogenic than that for galena. It is thus likely that the clastic sequence of the Proterozoic Kunyang Group is the source of ore metals in the Huize deposit. Leaching experimental results indicate that Pb and Zn in the clastic rocks are easily accessible, and the leaching by 10% HCl resulted in the preferential release of common Pb in leachates which have $^{206}Pb/^{204}Pb$ of 18.305–18.785, $^{207}Pb/^{204}Pb$ of 15.629–15.714, and $^{208}Pb/^{204}Pb$ of 37.695–38.593, similar to the ratios for galena. The thick clastic sequence of Proterozoic Kunyang Group is therefore the predominant source of ore metals in the Huize deposit. Precipitation of sulfides from ore-forming fluids resulted from secular interaction of deep-circulated fluid and the Kunyang Group in a relatively short ore-forming process may be the major reason for the nearly constant Pb isotope signatures of the Huize Zn-Pb deposit and insignificant contribution of the host rocks.

1. Introduction

The contiguous area of the Sichuan-Yunnan-Guizhou provinces in SW China, denoted as the Sichuan-Yunnan-Guizhou (SYG) triangle district in Chinese literature, is the most important Zn and Pb metallogenic district in China with more than 400 Mississippi Valley-type (MVT) Zn-Pb ore deposits in the southwestern margin of the Yangtze Block (Fig. 1). Among them, the Huize deposit is the largest MVT deposit in the southwestern margin of the Yangtze Block, with a total Pb and Zn reserve of about 7 Mt grading 25–35% Pb + Zn, and up to 60% Pb and Zn in places. In addition, the ores also contain economically significant Ag, Cd, In, Ge and Ga (Han et al., 2012, 2007; Huang et al., 2004; Luo et al., 2012; Zhang et al., 2015). The deposit has been the focus of intensive investigations ever since it was first exploited in the early 1950s (e.g., Hu and Zhou, 2012; Li et al., 2015; Wu et al., 2013; Zhang et al., 2005; Zhou et al., 2001, 2013a).

It is widely accepted that ore metals in the hydrothermal fluids of MVT deposits are mainly leached from the strata in the basin or from underlying basement rocks along the flow paths (Leach et al., 2010b). Ore metals in MVT Pb-Zn deposits can be derived from various source lithologies that are usually significantly older than the hydrothermal mineralization (Leach and Sangster, 1993), and reconstruction of possible Pb sources using Pb isotopes depends largely on the relative concentrations of Pb, U and Th in the source rocks and ages of mineralization (Schneider et al., 2002; Vaasjoki and Gulson, 1986). However, it is still enigmatic where such large amounts of Pb and Zn and other metals come from, as almost every geological unit in this region has been considered to be the source rocks in the literature; the carbonate sequences and Emeishan basalts were proposed to be the sources of ore metals based on the strata-bounded features of the deposit and high Pb and Zn contents of the carbonate rocks and basalts (Han et al., 2001; Huang et al., 2004; Li et al., 1999; Liu and Lin, 1999), whereas the host Carboniferous carbonates and the late Proterozoic igneous rocks were proposed because they have Pb isotopic compositions that overlapped
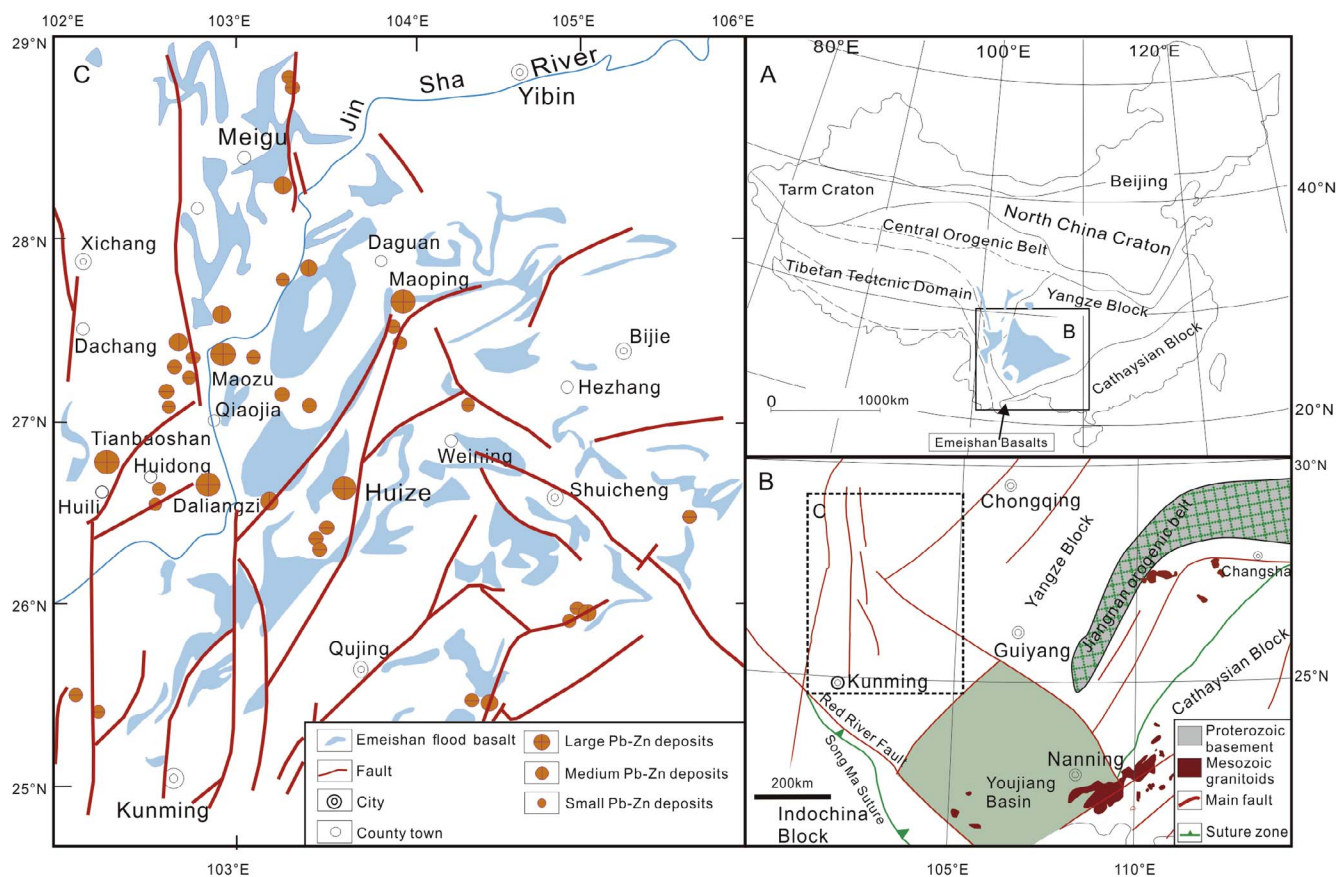

Fig. 1. Simplified tectonic and geological map of the Sichuan-Yunnan-Guizhou MVT ore province showing the geographic and tectonic locations (a, b) and distribution of the major ore deposits (c) [Modified after Liu and Lin (1999)]

with the ores (Li et al., 2007). In addition, some others favored a model of multiple sources including the basement, carbonate sequences, and the Emeishan basalts (Huang et al., 2003, 2004; Zhou et al., 2013b).

Lead isotopes can provide important insights into the source of metals and the interaction of hydrothermal fluids with specific rock types (Goldhaber et al., 1995; Slobodnik et al., 2008). It is thus
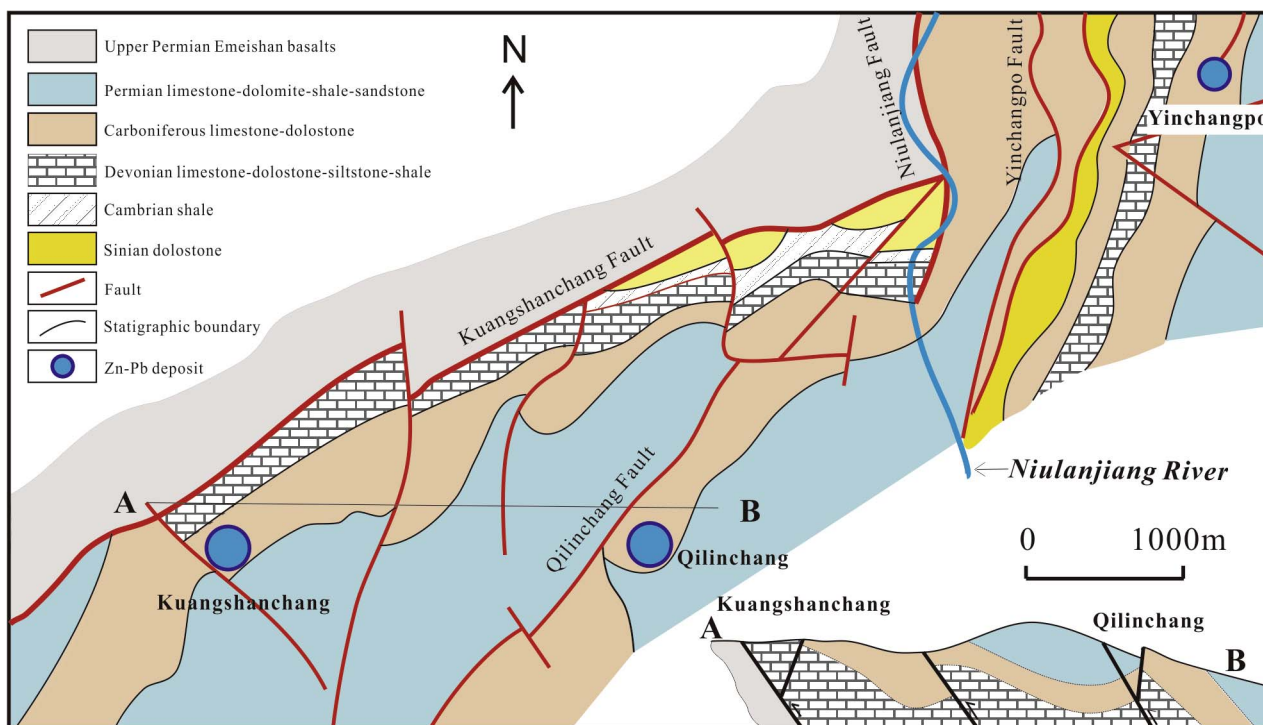

Fig. 2. Simplified geological map of the Huize deposit [Modified after Han et al. (2016)]
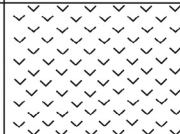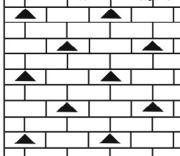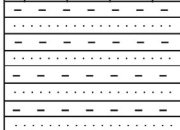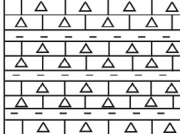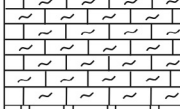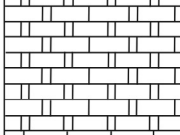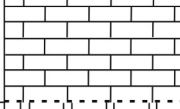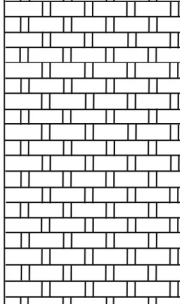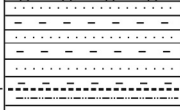
Epoch	Stratigraphic column	Thickness (m)	Lithological discriptions
Permian		600–800	The Emeishan basalts, gray to dark brown, mainly massive with locallized amygdaloidal and vesicular structures, discordant contact with underlain strata
		450–600	Pale to gray limestone or dolomitic limestone with interbedded dolostone, the dolomitic domains are commonly occur as irregular patches
		20–60	Carbonaceous shale intercalated with fine-grained sandstone in the upper part; yellowish fine-grained sandstone with interbedded brown argillite in the lower part
Carboniferous		27–85	Pisolitic limestone or limestone in the top part; purplish to yellowish green shale in the middle; and purplish breccioid limestone with argilaceous cement in the lower part
		10–20	Light gray limestone with interbedded oolitic limestone, and dolomitic limestone at the bottom
		40–60	Gray, yellowish, and pink coarse-grained dolostone with light gray limestone and dolomitic limestone interbeds. It is the main host rock, where orebodies arehosted in the pink coarse-grained dolostone.
		5–25	Gray aphanitic limestone and oolitic limestone; with 0-5 m thich of brownish siltstone and purplish mudstone at the top
Devonian		200–310	Gray aphanitic limestone, yellowish to pink middle-grained dolostone. The less importan host rock in the orefield.
			Light gray, middle- to thich-layered fine-grained dolostone, with locallized yellowish to light pink fine-grained dolostone at the top part.
			Light gray, middle to thick-layered fine- to middle-grained dolostone, and argilaceous dolostone interbeds are common in the middle to lower part.
		0–11	Light gray, yellowish intercalating sandstone, siltstone, and green to dark gray argillaceous shale; disconforitily contact with underlain sequences.
Cambrian		0–70	Dark argillaceous shale with interbedded yellowish sandy mudstone; disconformitily contact with underlain strata.
Sinian		>70	Pale siliceous dolostone, fault contact with underlain strata. The less important host rock in the orefield containing sulfide ore veins, and is believed to hold plausible prospecting potential at the depth and/or out of the Huize orefield.

Fig. 3. Schematic stratigraphic column for the Huize orefield showing the major facies and thickness of the sequences [after Li et al. (2006)]
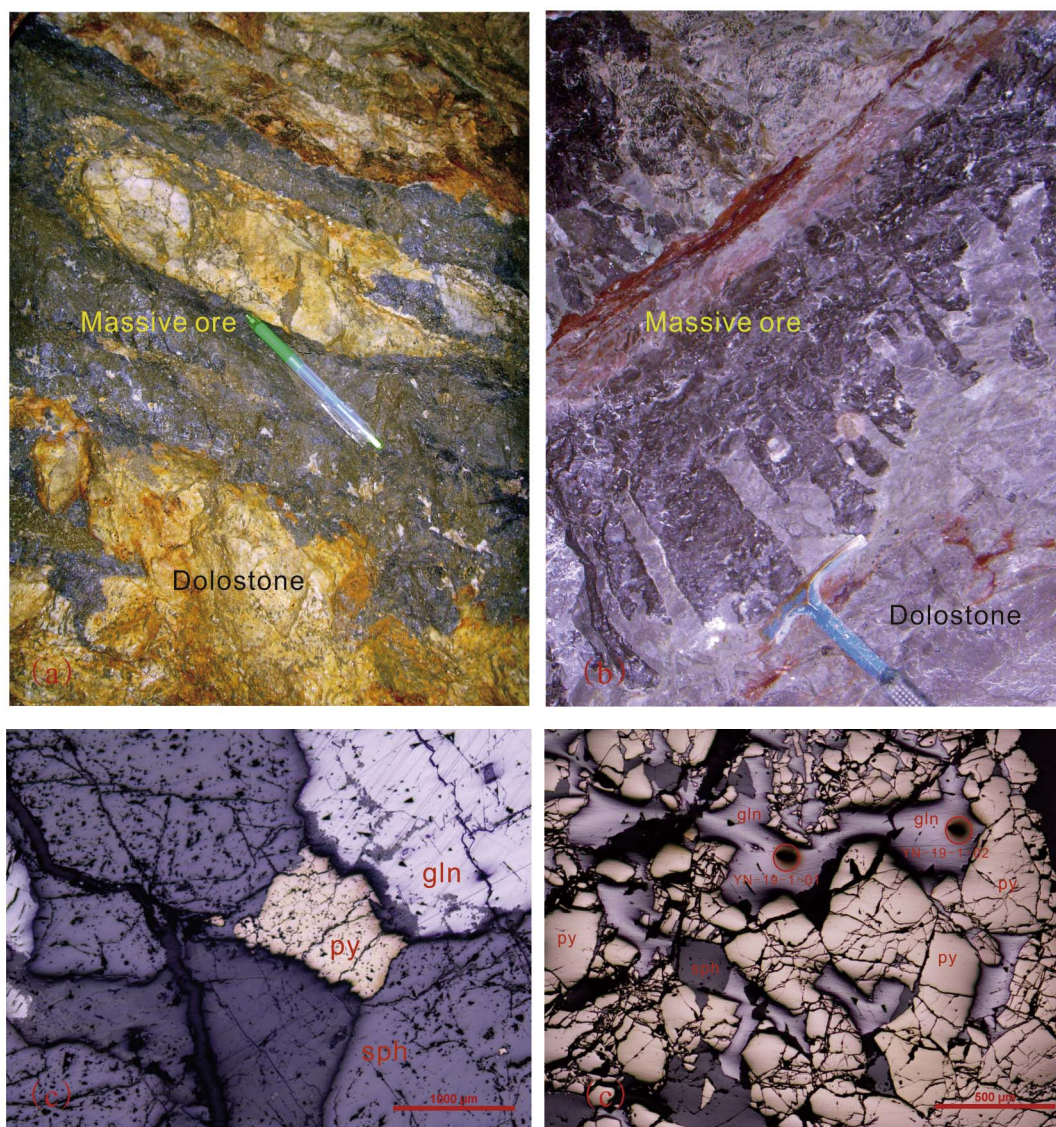
Fig. 4. Photos showing epigenetic features of ores (a, b) and ore mineral assemblages (c, d) [sph – sphalerite, py – pyrite, gln – galena; open circles in (d) are spots of *in situ* Pb isotope analysis]

commonly used to determine the sources of Pb (Pedersen, 2000; Portra and Moyers, 2017) and to guide exploration for some types of ore deposits (Gulson et al., 1986). A recently developed technique of *in situ* Pb isotope analyses using laser ablation inductively coupled plasma mass spectrometry (LA-ICPMS) and secondary ion mass spectrometry (SIMS) could resolve grain- and subgrain-scale isotopic variations, which are critical to complex textural relationships in ore systems. The technique also makes it possible to compare known chemical reservoirs and fluid sources by direct analysis for ore-forming minerals (Darling et al., 2012; Jin et al., 2016). The chalcophile features of Pb make it useful to trace the sources of hydrothermal deposits, especially for the MVT deposits in which Pb is an important ore metal.

In this study, we present *in situ* Pb isotopic compositions of galena from the Huize Zn-Pb deposit, and compare them with the Pb isotope data of the sedimentary rocks in this region. In addition, a preliminary leaching experiment was conducted on the possible source rocks to decipher the preferential leaching behavior of Pb isotopes. Our results indicate that the Proterozoic Kunyang Group is likely the metal source of the Huize Zn-Pb deposit. This conclusion will be applicable to other MVT deposits in this region.

2. Geological background

In SW China, the Yangtze Block is bounded by the Tibetan Plateau to the west, and the Indochina Block to the south. The Yangtze Block has a Mesoproterozoic to early Neoproterozoic basement which is locally unconformably overlain by the middle Neoproterozoic weakly metamorphosed strata and the late Neoproterozoic unmetamorphosed Sinian and Phanerozoic cover (Yan et al., 2003).

In the SYG triangle district, the basement consists mainly of Mesoproterozoic to the early Neoproterozoic (0.95–1.0 Ga) Kunyang Group. It is composed of sandstone, siltstone, slate, shale, dolostone, and minor tuffaceous volcanic rocks with a total thickness of about 20 km (Li et al., 1984), and experienced greenschist facies metamorphism. The Kunyang Group is considered to have deposited in a foreland basin setting (Ji et al., 2016; Li et al., 2013; Pang et al., 2015; Sun et al., 2009; Zhao et al., 2010). The overlying sedimentary strata are composed of Neoproterozoic to the middle Triassic submarine carbonate and clastic sedimentary sequences in a passive continental margin, and the late Triassic to Cenozoic terrigenous sedimentary sequences. Contact relationships among the rocks of different period are either conformable or show parallel unconformity.
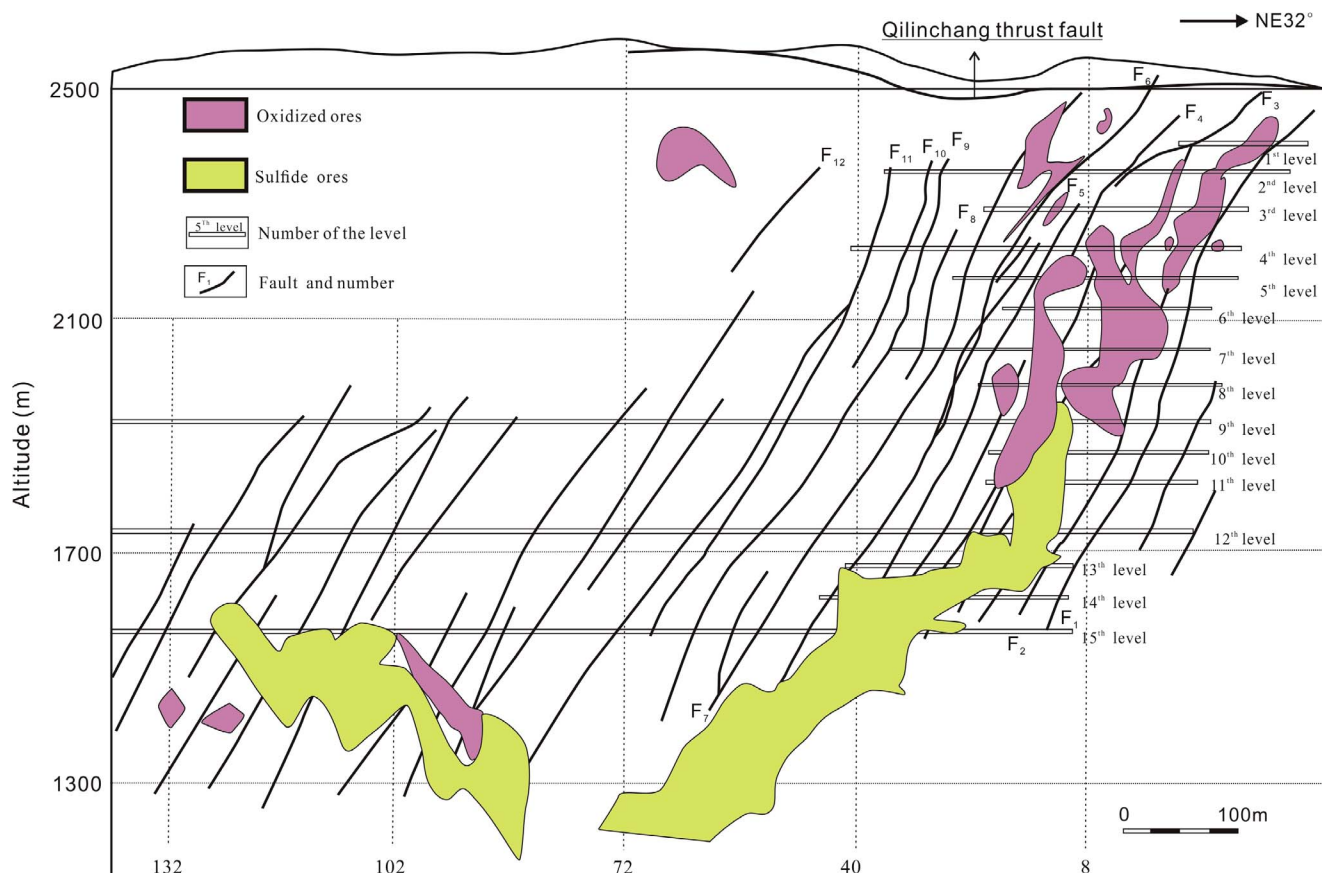
Fig. 5. Cross section profile of the Huize deposit [after Han et al. (2012)]

The Sinian System consists of mottled sandstone, tuffs and slate of the Chengjiang Formation, purplish tillite of the Nantuo Formation, neritic facies limestone and littoral facies clastic rocks of the Doushantuo Formation, and epicontinental dolostones of the Dengying Formation. The dolostone of the Dengying Formation is about 1 km in thickness and is the major rocks that host Pb-Zn deposits in this region.

A series of littoral to neritic facies sedimentary rocks composed of sandstone, shale, limestone had deposited in this region in Paleozoic, which were then overlain by voluminous flood basalts of the Emeishan large igneous province in the late Middle Permian with a peak age dated to be 259 ± 1 Ma (Ali et al., 2005; Shellnutt and Wang, 2014; Shellnutt et al., 2008; Zhong et al., 2014).

The Carboniferous Baizuo Formation is 60–277 m in thickness and consists of pale to reddish coarse-grained dolostones with interbedded limestone and siliceous limestone in local places. The upper Devonian Zaige Formation has a thickness of 40–60 m and consists mainly of light gray coarse-grained dolostone with intercalated siliceous limestone (Chen and Li, 2005; Meng, 2014; Zhong et al., 2013; Zhou et al., 2001). They are also major ore-bearing strata in the region.

Subsequent depositions in the region include Triassic siltstone and shale, and Jurassic to Cenozoic fluvial and lacustrine clastic rocks, mudstone, and freshwater marls.

The majority of Zn-Pb deposits are hosted in the rocks underlying the Emeishan flood basalts. The ore deposits that are hosted in the dolostones of the Dengying and Baizuo Formations account for about 81% of the proven Zn + Pb reserves in the SYG district (Chen, 2015; Liu, 1995; Liu and Lin, 1999).

3. The Huize Zn-Pb deposit

The Huize Zn-Pb deposit consists of three mines, *i.e.*, Qilinchang, Kuangshanchang, and Yinchangpo, which are separated by three NE-

striking thrust faults, namely the Kuangshanchang, Qilinchang, and Yinchanggou faults (Fig. 2). Mining operation in this region can be traced back to the Han Dynasty (decades before B.C.), and recent geological exploration has been carried out since 1950s.

More than 300 discrete ore bodies with Pb + Zn reserves ranging from ten to million tonnes have been found in the deposit. The ore bodies usually occur at the junction areas where NE-, NS- and NW-trending faults intersected and bounded by the Xiaojiang deep-seated fault zone to the west and the Zhaotong-Qujing concealed fault zone to the east. Overall, all the orebodies occur in the eastern flank of the Jinniuchang-Kuangshanchang anticline.

Most orebodies are mainly hosted in the dolostones of Carboniferous Baizuo Formation (Fig. 3), and others in Devonian Zaige Formation (Chen and Li, 2005; Meng, 2014; Zhong et al., 2013; Zhou et al., 2001). The ore bodies are commonly enveloped in coarse-grained dolostone and mainly distributed within the interstratified fault zone within the strata of the Baizuo Formation. Alteration of the host rocks is insignificant, and the orebodies have sharp contact with the host rocks, and often exhibit open-space filling features typical of MVT deposits (Leach et al., 2010a; Leach and Sangster, 1993). The weak alteration associated with Zn-Pb mineralization include dolomitization, silicification, carbonatization and pyritization. Ore bodies appear as tube-, lens- and column-like in shape, or as veins or veinlets in local places. An individual orebody can be 10– > 1000 m wide, 2–40 m thick and 800– > 1000 m long, and the thickness and grade of the ore bodies increase with the depth (Li et al., 2006).

The ores can be divided into three types, i.e., massive-, disseminated- and vein-type ores. The ores consist mainly of sphalerite, galena, pyrite, chalcopyrite, hopeite, matildite, acanthite, and freibergite, and gangue minerals include calcite and dolomite, with minor barite, gypsum, quartz and clay minerals (Fig. 4). Sphalerite is the dominant ore mineral in both massive and disseminated ores (Han

Table 1

fLA-MC-ICP-MS in-situ analytical results of Pb isotope compositions of galena from the Huize ore deposit.

Sample No.	H (m)[1]	Ore-type	$^{206}Pb/^{204}Pb$	1	$^{207}Pb/^{204}Pb$	1	$^{208}Pb/^{204}Pb$	1	t(Ma)[2]	μ
YN-14-01	1880	Massive/oxidized	18.4893	0.0007	15.7418	0.0008	38.9668	0.0024	283	9.73
YN-14-02	1880	Massive/oxidized	18.4899	0.0011	15.7399	0.0012	38.9522	0.0033	280	9.73
YN-14-03	1880	Massive/oxidized	18.4889	0.0016	15.7379	0.0015	38.9135	0.0041	279	9.73
YN-30-01	1864	Massive/oxidized	18.5084	0.0094	15.7679	0.0080	39.0524	0.0198	300	9.78
YN-30-02	1864	Massive/oxidized	18.5060	0.0016	15.7610	0.0017	39.0268	0.0045	294	9.77
YN-30-03	1864	Massive/oxidized	18.5004	0.0021	15.7551	0.0022	39.0098	0.0061	291	9.76
YN-5-2-01	1760	Disseminated	18.5007	0.0033	15.8058	0.0034	39.0070	0.0096	350	9.86
YN-5-2-02	1760	Disseminated	18.5049	0.0026	15.7647	0.0028	39.0308	0.0075	299	9.78
YN-2-2-01	1759	Massive	18.4989	0.0023	15.7593	0.0024	39.0131	0.0066	297	9.77
YN-7-01	1759	Massive	18.5264	0.0018	15.7647	0.0019	39.0737	0.0054	284	9.78
YN-4-01	1757	Disseminated	18.5069	0.0025	15.7671	0.0026	39.0358	0.0070	301	9.78
YN-9-1-01	1698	Massive	18.5043	0.0019	15.7686	0.0020	39.0389	0.0056	304	9.79
YN-9-1-02	1698	Massive	18.5041	0.0021	15.7706	0.0022	39.0424	0.0060	307	9.79
YN-9-1-03	1698	Massive	18.5031	0.0022	15.7669	0.0022	39.0375	0.0061	303	9.78
YN-10-2-01	1684	Massive	18.5012	0.0018	15.7657	0.0019	39.0254	0.0054	303	9.78
YN-10-2-02	1684	Massive	18.4964	0.0017	15.7608	0.0019	39.0189	0.0061	301	9.77
YN-12-1-01	1680	Massive	18.5035	0.0019	15.7702	0.0020	39.0357	0.0055	307	9.79
YN-12-1-02	1680	Massive	18.5011	0.0019	15.7668	0.0020	39.0251	0.0057	304	9.78
YN-12-1-03	1680	Massive	18.4857	0.0040	15.7473	0.0038	38.9701	0.0105	292	9.75
YN-12-1-04	1680	Massive	18.5036	0.0035	15.7652	0.0035	39.0144	0.0100	301	9.78
YN-12-2-01	1680	Massive	18.5058	0.0028	15.7531	0.0031	39.0142	0.0093	285	9.76
YN-13-01	1680	Massive	18.5068	0.0022	15.7727	0.0022	39.0470	0.0063	307	9.79
YN-21-1-01	1256	Massive	18.5005	0.0034	15.7668	0.0031	39.0337	0.0078	305	9.78
YN-21-1-02	1256	Massive	18.4988	0.0025	15.7676	0.0024	39.0330	0.0064	307	9.78
YN-21-2-01	1256	Massive	18.5010	0.0017	15.7635	0.0016	39.0289	0.0045	301	9.78
YN-21-2-02	1256	Massive	18.5061	0.0022	15.7666	0.0022	39.0388	0.0058	301	9.78
YN-22-1-01	1248	Massive	18.5092	0.0068	15.7777	0.0059	39.0467	0.0150	311	9.80
YN-22-1-02	1248	Massive	18.4977	0.0017	15.7663	0.0017	39.0251	0.0048	306	9.78
YN-22-2-01	1248	Massive	18.4943	0.0021	15.7601	0.0022	39.0044	0.0061	301	9.77
YN-22-2-02	1248	Massive	18.4912	0.0017	15.7559	0.0018	38.9954	0.0051	298	9.76
YN-29-01	1237	Massive	18.4979	0.0019	15.7618	0.0019	39.0153	0.0052	301	9.77
YN-29-02	1237	Massive	18.4940	0.0012	15.7580	0.0013	39.0023	0.0036	299	9.77
YN-29-03	1237	Massive	18.4969	0.0020	15.7613	0.0020	39.0153	0.0053	301	9.77
YN-25-01	1228	Vein	18.5022	0.0023	15.7676	0.0023	39.0298	0.0064	304	9.78
YN-25-02	1228	Vein	18.5042	0.0029	15.7690	0.0028	39.0375	0.0073	305	9.79
YN-26-01	1228	Vein	18.5089	0.0018	15.7573	0.0018	39.0347	0.0050	288	9.76
YN-18-1-01	1199	Massive	18.5073	0.0019	15.7612	0.0021	39.0296	0.0059	293	9.77
YN-15-1-01	1197	Massive	18.5013	0.0017	15.7635	0.0019	39.0165	0.0054	300	9.78
YN-15-1-02	1197	Massive	18.5025	0.0017	15.7657	0.0018	39.0249	0.0052	302	9.78
YN-15-1-03	1197	Massive	18.5000	0.0024	15.7609	0.0026	39.0050	0.0075	298	9.77
YN-19-1-01	1179	Massive	18.5085	0.0022	15.7722	0.0023	39.0492	0.0062	305	9.79
YN-19-1-02	1179	Massive	18.5079	0.0025	15.7741	0.0025	39.0517	0.0069	308	9.80
YN-19-2-01	1179	Massive	18.4909	0.0021	15.7577	0.0023	38.9984	0.0062	301	9.77
YN-19-2-02	1179	Massive	18.4934	0.0018	15.7581	0.0019	39.0002	0.0054	299	9.77
YN-33-1-01	1091	Disseminated	18.5186	0.0024	15.7728	0.0023	39.0670	0.0063	299	9.79
YN-33-1-02	1091	Disseminated	18.5178	0.0023	15.7733	0.0023	39.0668	0.0061	300	9.79
YN-33-1-03	1091	Massive	18.5217	0.0022	15.7755	0.0023	39.0756	0.0062	300	9.80
YN-33-2-01	1091	Massive	18.4901	0.0092	15.7524	0.0079	39.0102	0.0199	295	9.76
YN-33-2-02	1091	Massive	18.5070	0.0019	15.7630	0.0020	39.0354	0.0055	296	9.77
YN-33-2-03	1091	Massive	18.5082	0.0017	15.7619	0.0018	39.0325	0.0050	294	9.77

[1] Altitude above sea level.
[2] Pb isotope model age.

et al., 2007). The ores in the upper part of the deposit were oxidized by supergene fluids (Fig. 5). The oxidized ores are commonly yellowish to dark brown with complex mineral assemblage including smithsonite, galmey, hydrozincite, willemite, cerussite, sardinianite, limonite, and sulfide relics.

4. Analytical methods

The ore samples in this study were collected from underground mine, most samples were from the adits at interval of 1880–1191 m above sea level in the Qilinchang mine. The samples of the Kunyang Group and host rocks were collected in the places miles away from the orefield to avoid possible hydrothermal overprints related to the mineralization.

4.1. In situ Pb isotope analysis for galena

The galena was analyzed on the double side-polished slices of the ores using a 266 nm femtosecond laser-ablation multi-collector inductively coupled plasma mass spectrometry (fs-LA-MC-ICP-MS) at the State Key Laboratory of Continental Dynamics, Northwest University in China. The equipment consists of the Nu Plasma II MC-ICP-MS by Nu Instruments (Nu Ins, UK) and coupled 266-nm NWR UP Femto (ESI, USA) laser ablation system. To eliminate any potential contamination, the surfaces of the slices were carefully cleaned using anhydrous ethanol prior to laser ablation analysis. Test spots were carefully chosen to avoid possible influence of inclusions and impurities (Fig. 4d). High-temperature-activated carbon was used to filter Hg contained in the carrier gas (argon and helium), which reduced the Hg background and lowered the detection limit. Fractionation and mass discrimination effects existing in the ICP-MS analytical processes were corrected using an internal Tl isotope reference NIST SRM997 in conjunction with an
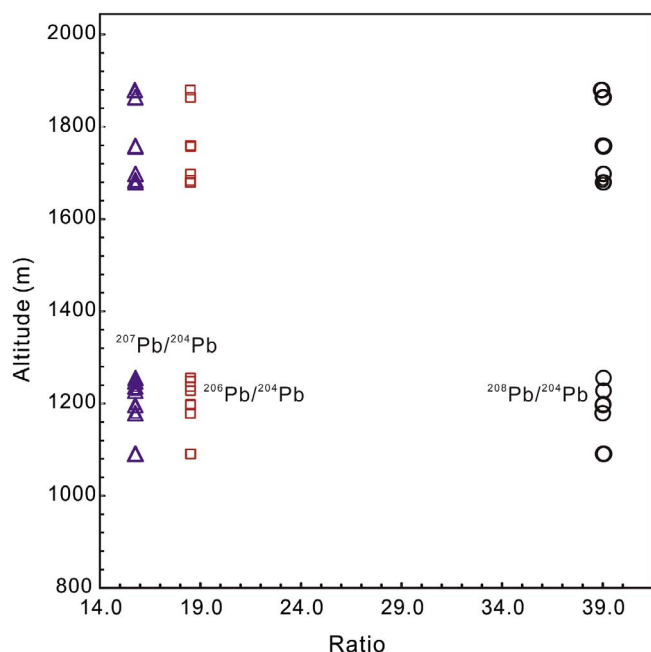
Fig. 6. Plot of ^{206}Pb/^{204}Pb, ^{207}Pb/^{204}Pb, and ^{208}Pb/^{204}Pb ratios vs. altitude of the samples showing extremely homogenous lead isotope signature of the Huize deposit.
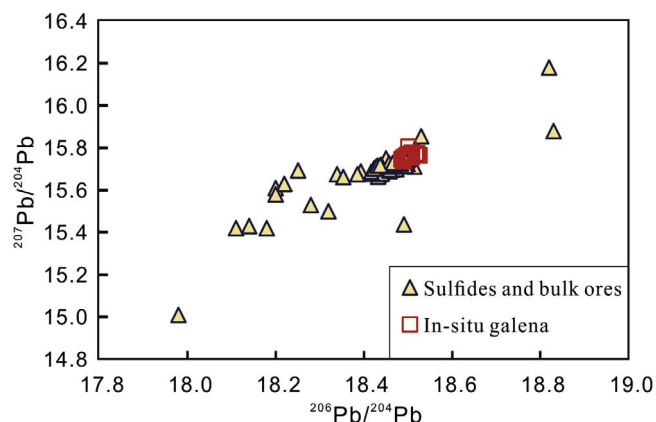

Fig. 7. ^{206}Pb/^{204}Pb vs. ^{207}Pb/^{204}Pb plot showing the difference between the previously published lead isotope compositions of sulfides and bulk ores and those of this study.

external reference NIST SRM 610, where the Tl solution is introduced through the CETAC Aridus II desolvation nebulizer system. The exponential law correction method for Tl normalization with optimum adjusted Tl ratio was utilized to obtain Pb isotopic data with good precision and accuracy. The measured isotopic ratios are in good agreement with the reference or published values within 2σ measurement uncertainties (Chen et al., 2014; Yuan et al., 2015).

4.2. Whole-rock Pb isotope analysis

Trace element concentrations and Pb isotope ratios of the Kunyang Group and host rocks were analyzed at the State Key Laboratory of Isotope geochemistry, Guangzhou Institute of Geochemistry, Chinese Academy of Sciences. Whole-rock samples were crushed in a steel crusher, carefully rinsed and powdered to < 200 mesh using an agate mill. The powdered samples were dried at 105 °C for 12 h before being analyzed.

Ore metals and trace elements of the samples were determined using a Perkin-Elmer Sciex ELAN 6000 ICP-MS at SKLIG. The powdered samples (50 mg) were dissolved in screw-top Teflon beakers using an HF + HNO$_3$ mixture for 7 days at ~100 °C. An internal standard

solution containing the single element Rh was used to monitor drift in mass response during counting. USGS standards BCR-1, W-2 and G-2 were used for calibrating element concentrations of the samples. In-run analytical precision for most elements is in a range of 2–5%. The detailed procedures for trace element analysis by ICP-MS were described by Li et al. (2002b).

Lead isotope measurements of whole-rock samples were obtained by using a Neptune Plus multiple collector inductively coupled plasma source mass spectrometer (MC-ICP-MS). 100 mg of rock powder was weighed into a Teflon vessel and dissolved in a HNO$_3$$^+$ HF mixture at 140 °C for 72 h. The solution was evaporated to dryness and then added with 2 ml concentrated HNO$_3$ and kept on an electric hot plate at 140 °C for 24 h. It was evaporated to dryness again and subsequently added 2 ml 6 M HCl and kept on a hot plate at 140 °C for another 24 h. It was finally dissolved in 0.8 M HBr solution in preparation for Pb purification. Pb was separated and purified by conventional anion exchange techniques (AG1X8, 200–400 resin) with dilute HBr as eluant. The total procedural blank is less than 0.4 ng. Samples are doped with Tl, and mass discrimination was corrected relative to a certified ^{205}Tl/^{203}Tl ratio. The detail analytical procedures are similar to those described by Baker and Waight (2002). During the period of analysis, repeated analyses of NBS981 yielded ^{206}Pb/^{204}Pb = 16.9368 ± 4 (2σ), ^{207}Pb/^{204}Pb = 15.4881 ± 5 (2σ), and ^{208}Pb/^{204}Pb = 36.6788 ± 11 (2σ).

4.3. Leaching experiment

A tentative leaching experiment was carried out in this study to delineate the mobility of ore metals in the rocks and the variation of Pb isotope ratios in the leachate and bulk rock sample. 1 g of powdered samples of possible source rocks was carefully weighed to centrifuge tubes, 5 ml 10% HCl was added and shacked for 30 min in an ultrasonic vibration instrument. For the organic-rich rocks such as black shale and carbonaceous slate, excessive H$_2$O$_2$ was added to dissolve the organics before leaching. After 24 h' resting, the tubes were transferred to a centrifugal machine, then centrifuged for 10 min, and the liquids were filtered and decanted into new centrifuge tubes. The residuals were rinsed with MILIQ water, centrifuged and integrated to the leachates for five times. The ore metal and trace element concentrations and Pb isotopes of the leachates were analyzed using ICP-MS and MC-ICP-MS methods following procedures described above.

5. Results

5.1. Mineral and whole-rock Pb isotopic compositions

The galena grains analyzed in this study have restricted Pb isotopic compositions with ^{206}Pb/^{204}Pb of 18.486–18.526, ^{207}Pb/^{204}Pb of 15.738–15.806, and ^{208}Pb/^{204}Pb of 38.914–39.076 (Table 1). The galena grains in different ore types at different altitudes have similar Pb isotopic compositions (Fig. 6). Compared with the results in this study, the Pb isotopic compositions of the sulfides reported in earlier studies and analyzed by conventional method are much scattered (Han et al., 2007; Li et al., 2007; Zhou et al., 2001) (Fig. 7). This is possibly because *in situ* determination can effectively avoid the influences of impurities in sulfides and errors introduced during chemical preparations.

The Pb isotopic compositions of the galena in this study are plotted just above the average crustal growth curves (Zartman and Haines, 1988) in the plots of ^{207}Pb/^{204}Pb versus ^{206}Pb/^{204}Pb and ^{208}Pb/^{204}Pb versus ^{206}Pb/^{204}Pb (Fig. 8), whereas the samples of the country rocks including those from the Kunyang Group, Baizuo Formation, Dengying Formation, and the Emeishan flood basalts have highly variable Pb isotopic compositions (Table 2). The dolostones of the Baizuo and Dengying Formation and the Emeishan flood basalts have ^{206}Pb/^{204}Pb varying from 19.430 to 23.974, ^{207}Pb/^{204}Pb from 15.764 to 16.046 and ^{208}Pb/^{204}Pb from 38.814 to 42.975, which are remarkably different
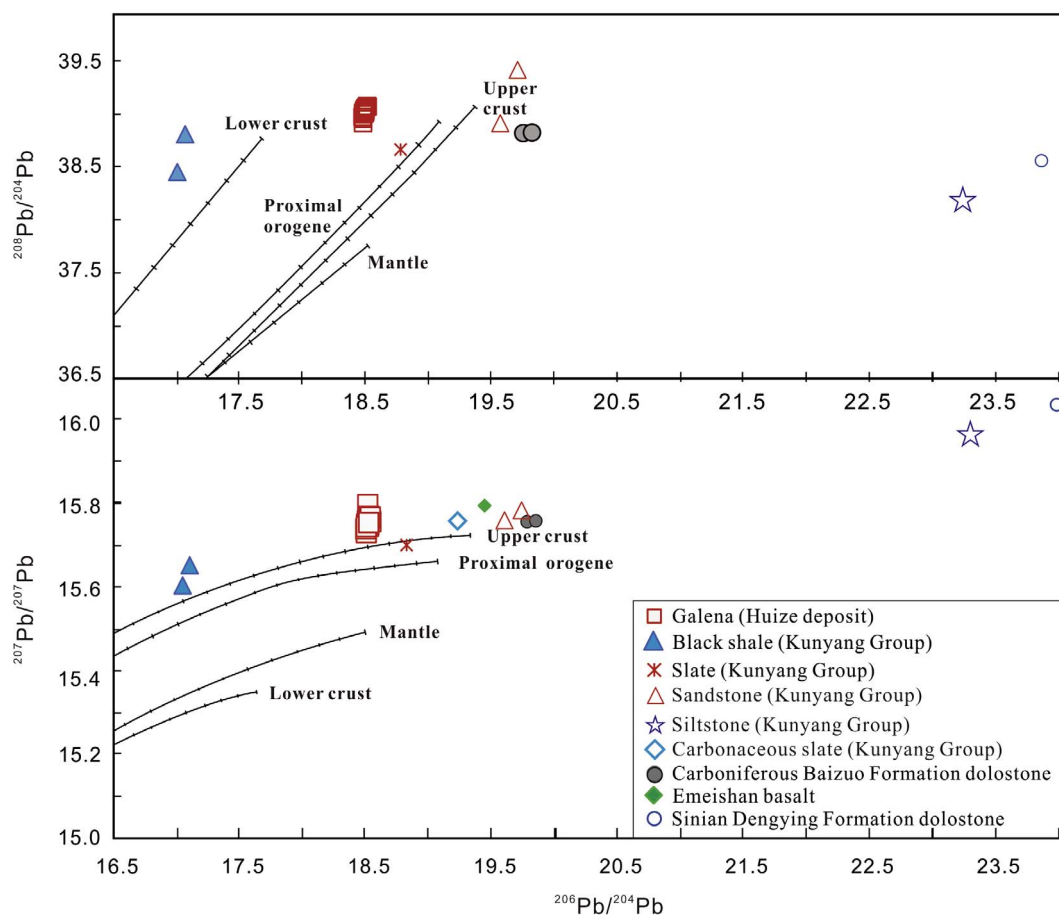
Fig. 8. Lead isotope composition of galena from the Huize deposit and the basement and host rocks in this study. Pb isotope evolution curves for designated model reservoirs are after Zartman and Haines (1988) and Pb isotope compositions of the whole rocks are age-corrected.

from that of galena. On the other hand, the clastic rocks of the Kunyang Group have $^{206}Pb/^{204}Pb$ of 18.7891–23.2739, $^{207}Pb/^{204}Pb$ of 15.7121–16.0050, and $^{208}Pb/^{204}Pb$ of 38.1689–39.4102, similar to the ratios for the galena in the ores of the Huize Zn-Pb deposit.

5.2. Leaching experimental results

The clastic rocks of the Kunyang Group contain 100 ppm Pb and 200 ppm Zn, much higher than those for other sedimentary rocks in this region (Zhang, 2009). In addition, they have similar Pb isotopic compositions to the galena from the Huize deposit. They are therefore selected for the leaching experimental study. The results indicate that leachates of the organic-rich and -poor clastic rocks have disparate Pb isotope features.

The leachates of organic-poor sandstone, siltstone and slate are obviously less radiogenic than those of the whole-rock samples, whereas the leachates of organic-rich black shale and carbonaceous slate are much radiogenic than those for the whole-rock samples (Table 3; Figs. 9 and 10). The less radiogenic Pb in the leachates of organic-poor clastic rocks indicates that the radiogenic Pb in the organic-poor rocks is likely hosted in the insoluble phases such as silicates and U- and Th-rich accessary minerals, whereas the common Pb mainly occur in carbonates and/or calcareous cement. Therefore, progressive interaction of the rocks and acid hydrothermal fluids could result in the release of more radiogenic Pb from these rocks, so that the leachates may have Pb isotope features similar to that for the galena of the ores.

On the other hand, the leachates of organic-rich black shale and carbonaceous slate have highly radiogenic Pb isotopic compositions

Table 2
Lead isotope compositions of the rocks in the Huize orefield and neighbor region.

Period	Rock	Th(ppm)	U(ppm)	Pb(ppm)	$(^{206}Pb/^{204}Pb)^*$	$(^{207}Pb/^{204}Pb)^*$	$(^{208}Pb/^{204}Pb)^*$
Mesoproterozoic Kunyang Group	Black shale	6.56	39.7	50.6	17.0702	15.6604	38.8043
		6.56	39.7	50.6	17.0087	15.6102	38.4424
	Carbonaceous slate	17.9	3.15	7.25	19.2291	15.7735	36.3521
	Slate	6.73	8.62	21.4	18.7891	15.7121	38.6896
	Siltstone	3.88	1.73	8.18	23.2739	16.0050	38.1689
	Thick-layered sandstone	4.50	1.66	4.47	19.7253	15.7841	39.4102
	Middle-layered sandstone	7.25	2.48	7.96	19.5817	15.7615	38.9334
Sinian Dengying Formation	Dolostone	0.08	0.249	6.95	23.9736	16.0464	38.4842
Carboniferous Baizuo Formation	dolostone	0.151	0.366	2.36	19.7671	15.7640	38.8143
	dolostone	0.151	0.366	2.36	19.8362	15.7661	38.8206
Permian	Emeishan basalt	2.54	2.59	3.36	19.4296	15.8027	42.9747

* Represent radiogenic lead corrected ratios.

Table 3
Ore metal contents and Pb isotopic composition of the whole rocks of the Kunyang Group and their 10% HCl leachates.

Sample	Th	U	Pb	Zn	$^{206}Pb/^{204}Pb$	$^{207}Pb/^{204}Pb$	$^{208}Pb/^{204}Pb$	$(^{206}Pb/^{204}Pb)^{*}$	$(^{207}Pb/^{204}Pb)^{*}$	$(^{208}Pb/^{204}Pb)^{*}$
Back shale	6.56	39.68	50.57	15.68	18.6574	15.7400	38.8899	17.0702	15.6604	38.8043
Back shale	6.56	39.68	50.57	15.68	18.5857	15.6893	38.5274	17.0087	15.6102	38.4424
10% HCl leachate	0.91	19.51	19.24	4.16	23.1391	15.9869	38.4317	20.3734	15.8483	38.1771
Carbonaceous slate	17.89	3.15	7.25	76.90	20.1164	15.8180	37.9943	19.2291	15.7735	36.3521
10% HCl leachate	1.41	0.20	4.11	28.87	19.7410	15.7847	41.1382	19.5061	15.7730	41.0424
Slate	6.73	8.62	21.42	27.84	19.6135	15.7534	38.8996	18.7891	15.7121	38.6896
10% HCl leachate	0.17	0.31	10.81	2.04	18.9289	15.7213	37.7270	18.7848	15.7141	37.6949
Siltstone	3.88	1.73	8.18	12.44	23.7312	16.0279	38.5027	23.2739	16.0050	38.1689
10% HCl leachate	0.00	0.00	0.07	0.64	18.7382	15.6698	38.5934	18.6496	15.6654	38.5934
Sandstone	7.25	2.48	7.96	301.20	20.2322	15.7941	39.5521	19.5817	15.7615	38.9334
10% HCl leachate	0.19	0.05	2.48	133.28	18.4404	15.6354	38.1041	18.3049	15.6286	38.0501

Ore metal contents listed are represented as µg/g (whole rock powder).
  * Radiogenic corrected ratios.
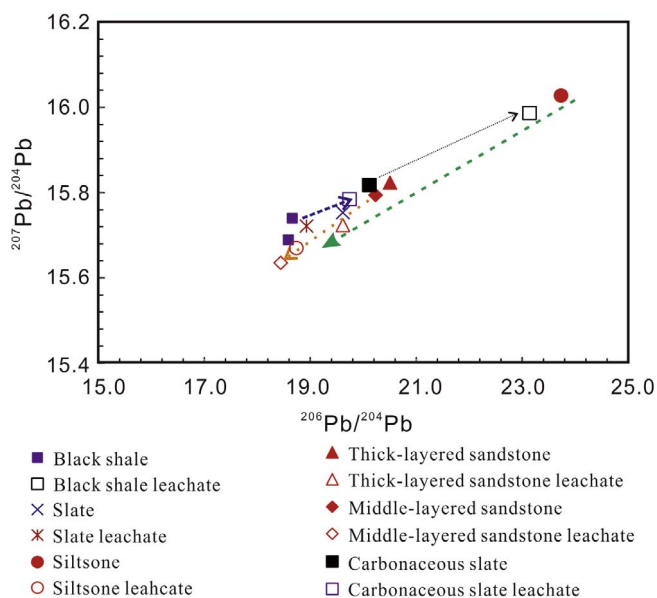

Fig. 9. $^{206}Pb/^{204}Pb$ vs. $^{207}Pb/^{204}Pb$ plot of the previously published data of the Kunyang Group and host rocks.

and contain high U and Th contents which may be absorbed in the organics during sedimentation and diagenesis. The organic matters in these rocks may absorb and retrain the releasing of ore metals from rocks during water-rock interactions (Davis, 1984; Reuter and Perdue, 1977). The significant differences between the leachates of organic-rich rocks and galena demonstrate that the contribution of the black shale and carbonaceous slate was much less important if any.

6. Discussion

6.1. Comparison of the Pb isotope data obtained in this study and literature

Lead is the predominant metal component of galena, and the tendency for galena to exclude the parent isotopes of U and Th make Pb isotope ratios of galena close to initial values at the time of crystallization, and no correction for radiogenic in-growth is required. *In situ* Pb isotope analyses of galena indicate that the ores in the deposit have very narrow ranges of Pb isotope compositions, which is strikingly in contrast with those of the previously published results on the ores. The previously published Pb isotope data of the ores from the Huize deposit as well as the Kunyang Group and host rocks in the region are widely scattering (Fig. 11). It is noteworthy that most of rock samples in the previous works were collected from the mining areas and the results are commonly not age-corrected for the radiogenic Pb daughter isotopes
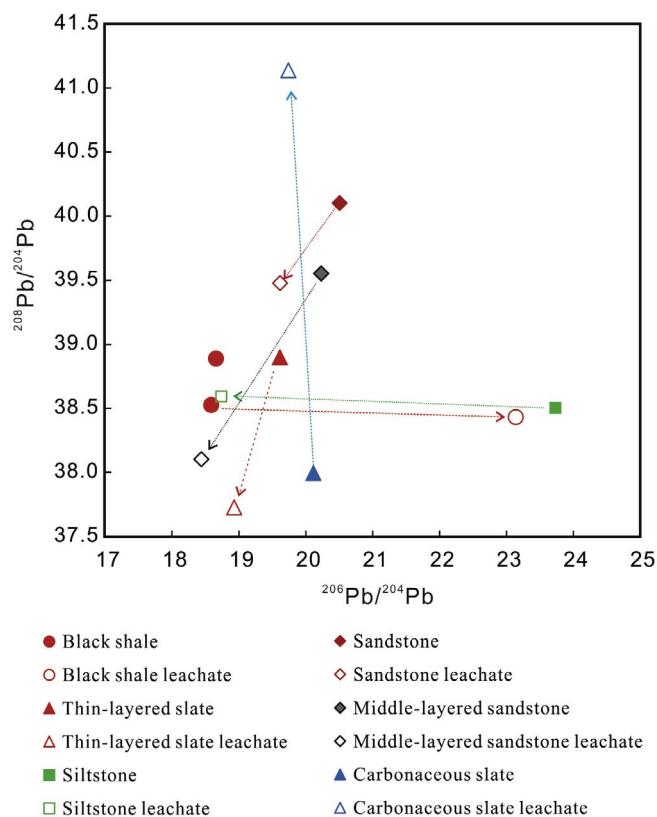

Fig. 10. $^{206}Pb/^{204}Pb$ vs. $^{207}Pb/^{204}Pb$ plot of the bulk rocks and leachates. Acidic solution (10% HCl) preferentially leaches common lead in the clastic rocks, but radiogenic Pb in the organic rich sedimentary rocks.

due to the lack of U, Th and Pb data. The highly overlapping ranges of Pb isotopic compositions for the ores and rocks are likely resulted from poor precision of the less advanced analytical techniques in the last century, impurity of sulfide separates, and not age-corrected data, and consequently almost all of the rock units were proposed by different researchers to be the source rocks of the Zn-Pb ore mineralization.

6.2. Uniform Pb isotope of the galena

The Pb isotopic homogeneity of the Huize deposit is strikingly in contrast with the typical MVT deposits in the US, which commonly have distinctive Pb isotope compositions in sulfides of different generation and even in single crystal which is commonly believed to be results of mixing of multiple sources (e.g., Crocetti et al., 1988; Deloule et al., 1986; Foley et al., 1981; Sverjensky, 1981). The homogeneity of
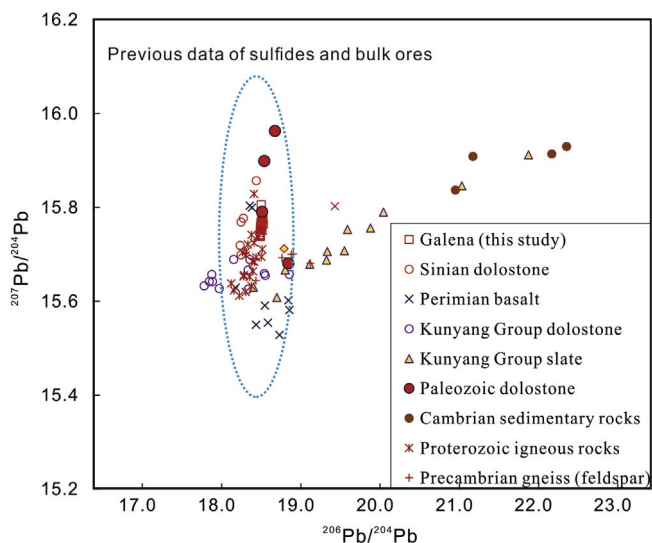
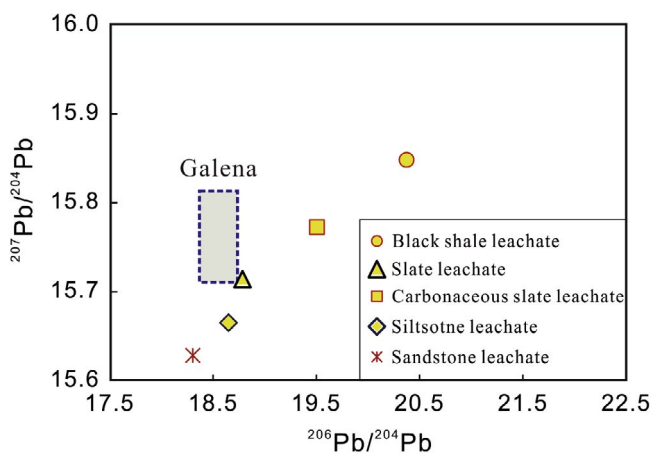**Fig. 11.** $^{206}Pb/^{204}Pb$ vs. $^{208}Pb/^{204}Pb$ plot of the bulk rocks and leachates.

Fig. 12. $^{206}Pb/^{204}Pb$ vs. $^{207}Pb/^{204}Pb$ plot of lead isotope compositions of the galena and leachates (age-corrected values) of the Kunyang Group rocks.

Fig. 13. $^{206}Pb/^{204}Pb$ vs. $^{208}Pb/^{204}Pb$ plot of lead isotope compositions of the galena and leachates (age-corrected values) of the Kunyang Group rocks.
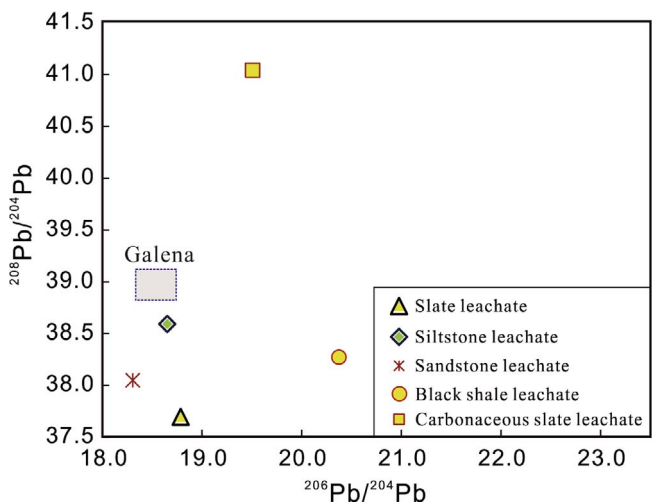
the isotopic composition of ores depends on the degree of mixing and homogenization of Pb prior to ore deposition. Leaching of Pb from thick sedimentary piles and/or basement rocks and the protracted

mechanical and/or chemical homogenization as well as the long distance lateral transportation were suggested to be responsible for uniform Pb isotope ratios in large deposits (Vaasjoki and Gulson, 1986; Wilkinson, 2014).

The homogenous Pb isotopic composition of the galena indicate that the ore metals in the Huize deposit Pb originated from a single or well-mixed source. The high $^{207}Pb/^{204}Pb$ and $^{208}Pb/^{204}Pb$ ratios (Fig. 8) may indicate ancient crustal source rocks and/or possibly lower crustal domains with elevated Th/U ratios (Schneider et al., 2002).

6.3. The Kunyang Group is the major source of ore metals

The Kunyang Group and host rocks have distinct Pb isotope compositions (age-corrected to 200 Ma) (Fig. 8). The Pb isotopes of the Permian Emeishan basalts, Carboniferous Baizuo Formation and Sinian Dengying Formation dolostones are significantly different from that of galena. In addition, the Paleozoic sedimentary rocks and Emeishan basalts have ore metal contents lower than or similar to their corresponding crustal abundances (Li et al., 2002a). Therefore, because the rocks are characterized by low ore metal contents, lack metamorphism and hydrothermal alteration, and Pb isotopic signatures distinct from the ores, it can be concluded that those rocks are unlikely the major source(s) of the ore metals.

Pb isotope compositions of the Proterozoic Kunyang Group rocks have a wide range of variation, however, the clastic rocks (sandstone-siltstone-slate) have Pb isotope compositions similar to that of the galena, only slightly more radiogenic (Fig. 8). Therefore, we assume that the clastic rocks of the Kunyang Group are probably the major source of the metals for the Huize Zn-Pb deposit.

Lead in rocks accessible to hydrothermal fluids and bulk rocks may differ considerably, while isotope compositions of leachable lead essentially depend on the mineralogical composition of the rocks; and it is evidenced that different phases of rocks commonly have significantly different Pb isotope compositions (e.g., Gulson, 1977; Macfarlane and Petersen, 1990; Pedersen, 2000). Thus, the slight radiogenic Pb isotopic feature of the organic-poor clastic rocks may be mitigated during water-rock interaction. And indeed, the leaching experiment shows that 10% HCl will preferentially leach common lead in the clastic rock of the Kunyang Group (Figs. 9 and 10), suggesting that hydrothermal solution may preferentially leach common lead from low-grade metasedimentary rocks, which is consistent with the results of Chiaradia and Fontbote (2003). In spite of the fact that the leachates of the clastic rocks are slightly less radiogenic than that of galena, the progressive hydrothermal fluid interaction will possibly elevate the radiogenic lead of the fluids to the ratios of the ores, and thus, the clastic rocks are the most possible source rocks for the mineralization (Figs. 12 and 13).

The clastic rocks in the Kunyang Group have a thickness of around 20 km (Li et al., 1984; Lv and Dai, 2001) and have average Pb and Zn contents of 100 ppm and 200 ppm, respectively (Zhang, 2009), which are favorable for the formation of the Huize Zn-Pb deposit. Our leaching experimental results demonstrate that the ore metals in the organic-poor clastic rocks are easily accessible to hydrothermal fluids, the sandstone in particular, 31% of the Pb and 44% of Zn can be extracted by 10% HCl solution (Table 3). The results imply that a substantial part of Pb and Zn in the organic–poor clastic rocks occur in carbonate phases and/or calcareous cements, which make the rocks plausible sources of ore metals. If we assume 5% of the clastic rocks in the Kunyang Group was involved in hydrothermal interaction, during which 20% of the zinc and lead will be released, while 25% of released metals will be precipitated during ore mineralization, and the density of the rocks at 2.5 t/m³, thus, less than 200 Km³ of such clastic rocks (the rocks within an area of less than 200 Km²) will supply enough ore metals for the formation of the Huize deposit.

In addition, feldspars from the Precambrian gneisses in the basement (He et al., 2015; Liu et al., 2000) and the whole rocks of Proterozoic igneous rocks in the region (Zhou et al., 1998) also have Pb
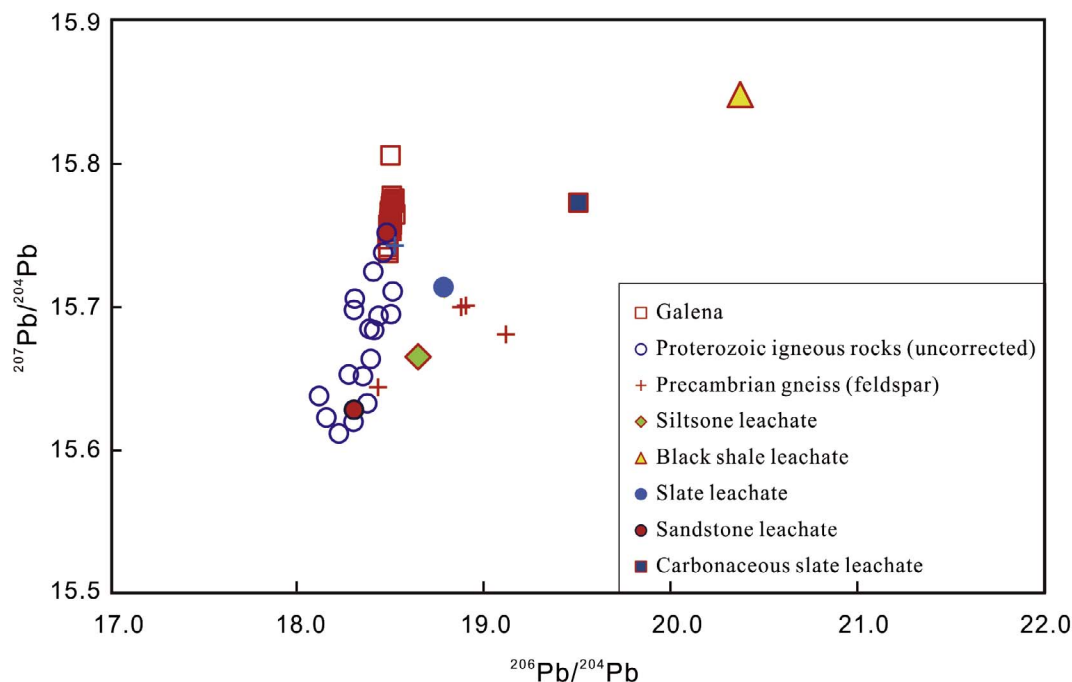
Fig. 14. $^{206}Pb/^{204}Pb$ vs. $^{207}Pb/^{204}Pb$ plot showing the similarity between Pb isotope composition of galena, age-corrected leachates of the Proterozoic Kunyang Group clastic rocks, Precambrian gneiss and Proterozoic igneous rocks.

isotope compositions similar to that of galena (Fig. 14). Considering that feldspar is the dominant Pb-bearing phase in igneous rocks (Housh and Bowring, 1991), and due to the low U/Pb and Th/Pb ratios, age-correction of its lead isotopic composition is unnecessary (Carignan and Gariepy, 1993). Previous leaching experiments demonstrated that feldspars contain radiogenic lead which can be removed preferentially to non-radiogenic lead (Housh and Bowring, 1991), therefore, preferential leaching of radiogenic lead from the Precambrian gneisses and the ore-metal rich Proterozoic granitic and rhyolitic volcanic rocks (Chen and Wu, 2012; Zhou et al., 2001) may also release Pb with Pb isotopes similar to that of the galena, and thus the contribution of the gneisses in the basement and the Proterozoic igneous rocks could not be excluded (Fig. 14).

Leaching of ore metals from the thick pile of ore metal rich clastic rocks in the Kunyang Group by the deep circulated hydrothermal fluids, which may also integrate with metals released from the Proterozoic igneous rocks and the Precambrian gneisses in the basement and homogenize through secular interaction and long distance migration, should be the key mechanism responsible for the ore mineralization. However, due to their localized distribution, contribution of the Proterozoic igneous rocks and Precambrian gneiss may be less important than that of the Kunyang Group clastic rocks. Involvement of basement rocks in the MVT systems has been speculated by many researchers based on isotopic evidence which suggests possible interactions between basement and hydrothermal fluids (Everett et al., 2003; Han et al., 2016; Koppel and Schroll, 1988; Luczaj et al., 2007; Shelton et al., 1995; Wilkinson, 2014; Zhou et al., 2001). Our results demonstrated that the Kunyang Group clastic rocks in the basement was the primary source of ore metals in the Huize deposit. The possible involvement of deeply circulating fluids in the basement is also supported by the high homogenization temperatures of fluid inclusions in sphalerite (can be up to > 280 °C, our unpublished data and Han et al. (2016)) which are significantly higher than normal hydrothermal fluids of MVT mineralization (Leach et al., 2005).

7. Conclusions

Pb isotope composition of galena from the Huize deposit is extremely homogenous, no significant variation has been observed in different ore types and spatially over 800 m vertically. Comparative source-rock Pb isotope analyses and leaching experiment show that the organic-poor clastic rocks in the Kunyang Group may be the predominant source of the ore metals, whereas the Proterozoic igneous rocks and Precambrian gneisses may also contribute to the ore mineralization. It can be inferred that formation of the Huize deposit was likely related the secular interaction between the deep-circulating fluids and the thick pile of ore metal rich clastic rocks, and the long distance migration of ore fluids resulted in extraction of abundant ore metals and homogenization of Pb isotopes of the ores.

Appendix A. Supplementary data

Supplementary data associated with this article can be found, in the online version, at http://dx.doi.org/10.1016/j.oregeorev.2017.08.019.

References

Ali, J.R., Thompson, G.M., Zhou, M.F., Song, X.Y., 2005. Emeishan large igneous province, SW China. Lithos 79 (3–4), 475–489.

Baker, J., Waight, T., 2002. Pb isotope analysis using Tl and a Pb-207-Pb-204 spike on a double focusing MC-ICPMS. Geochim. Cosmochim. Acta 66 (15a) A44-A44.

Carignan, J., Gariepy, C., 1993. Pb Isotope geochemistry of the silidor and launay gold deposits – Implications for the source of archean au in the abitibi subprovince. Econ. Geol. Bull. Soc. Econ. Geol. 88 (6), 1722–1730.

Chen, D., 2015. Space-time distribution, source bed and statabound mechanisms of Zn-Pb deposits in western margin of Yangtze platform. J. Jilin Univ.: Earth Sci. Ed. 45 (5),

1365–1383 (in Chinese with English abstract).

Chen, Y.S., Li, Y., 2005. Reasons of formation of Huize lead-zinc ore body. Min. Eng. 3 (6), 14–16 (in Chinese with English abstract).

Chen, D., Wu, L.F., 2012. Distribution and metallogeny of Pb-Zn deposits in the Sichuan-Yunnan-Guizhou boder region. Acta Geol. Sin. 32 (3), 304–308 (in Chinese with English abstract).

Chen, K.Y., Yuan, H.L., Bao, Z.A., Zong, C.L., Dai, M.N., 2014. Precise and accurate in situ determination of lead isotope ratios in NIST, USGS, MPI-DING and CGSG glass reference materials using femtosecond laser ablation MC-ICP-MS. Geostand. Geoanal. Res. 38 (1), 5–21.

Chiaradia, M., Fontbote, L., 2003. Separate lead isotope analyses of leachate and residue rock fractions: implications for metal source tracing in ore deposit studies. Miner. Deposita 38 (2), 185–195.

Crocetti, C.A., Holland, H.D., Mckenna, L.W., 1988. Isotopic composition of lead in galenas from the viburnum trend, Missouri. Econ. Geol. 83 (2), 355–376.

Darling, J.R., Storey, C.D., Hawkesworth, C.J., Lightfoot, P.C., 2012. In-situ Pb isotope analysis of Fe-Ni-Cu sulphides by laser ablation multi-collector ICPMS: New insights into ore formation in the Sudbury impact melt sheet. Geochim. Cosmochim. Acta 99, 1–17.

Davis, J.A., 1984. Complexation of trace-metals by adsorbed natural organic-matter. Geochim. Cosmochim. Acta 48 (4), 679–691.

Deloule, E., Allegre, C., Doe, B., 1986. Lead and sulfur isotope microstratigraphy in galena crystals from mississippi valley-type deposits. Econ. Geol. 81 (6), 1307–1321.

Everett, C.E., Rye, D.M., Ellam, R.M., 2003. Source or sink? An assessment of the role of the old red sandstone in the genesis of the Irish Zn-Pb deposits. Econ. Geol. Bull. Soc. Econ. Geol. 98 (1), 31–50.

Foley, N.K., Sinha, A.K., Craig, J.R., 1981. Isotopic composition of lead in the austinville-ivanhoe Pb-Zn district, Virginia. Econ. Geol. 76 (7), 2012–2017.

Goldhaber, M.B., et al., 1995. Lead and sulfur isotope investigation of Paleozoic sedimentary rocks from the southern midcontinent of the United States: Implications for paleohydrology and ore genesis of the southeast Missouri lead belts. Econ. Geol. Bull. Soc. Econ. Geol. 90 (7), 1875–1910.

Gulson, B.L., 1977. Lead isotope results of acid leaching experiments on acid volcanics and black shales in an ore environment. Geochem. J. 11 (4), 239–245.

Gulson, B.L., Vaasjoki, M., Carr, G.R., 1986. Geochronology in deeply weathered terrains using lead lead isochrons. Chem. Geol. 59 (4), 273–282.

Han, R.S., et al., 2001. Genesis modeling of Huize lead-zinc ore deposit in Yunnan. Acta Mineral. Sin. 21 (4), 674–680 (in Chinese with English abstract).

Han, R.S., et al., 2007. Geological features and origin of the Huize carbonate-hosted Zn-Pb-(Ag) District, Yunnan, South China. Ore Geol. Rev. 31 (1–4), 360–383.

Han, R.S., et al., 2012. Mineralization model of rich Ge-Ag-bearing Zn-Pb polymetallic deposit concentrated district in Northeastern Yunnan, China. Acta Geol. Sin. 86 (2), 280–294 (in Chinese with English abstract).

Han, R.S., et al., 2016. Infrared micro-thermometry of fluid inclusions in sphalerite and geological significance of Huize super-large Zn-Pb-(Ge-Ag) deposit, Yunnan Province. J. Jilin Univ.: Earth Sci. Ed. 46 (1), 91–104 (in Chinese with English abstract).

He, F., et al., 2015. Lead isotope compositions of Dulong Sn-Zn polymetallic deposit, Yunnan, China: Constraints on ore-forming metal sources. Acta Mineral. Sin. 35 (3), 309–319 (in Chinese with English abstract).

Housh, T., Bowring, S.A., 1991. Lead isotopic heterogeneities within alkali feldspars – Implications for the determination of initial lead isotopic compositions. Geochim. Cosmochim. Acta 55 (8), 2309–2316.

Hu, R.Z., Zhou, M.F., 2012. Multiple Mesozoic mineralization events in South China-an introduction to the thematic issue. Miner. Deposita 47 (6), 579–588.

Huang, Z.L., et al., 2003. Carbon and oxygen isotope constraints on mantle fluid involvement in the mineralization of the Huize super-large Pb-Zn deposits, Yunnan Province, China. J. Geochem. Explor. 78–9, 637–642.

Huang, Z.L., Li, W.B., Han, R.S., Chen, J., 2004. Several problems involved in genetic studies on Huize superlarge Pb-Zn deposit, Yunnan Province. Acta Mineral. Sin. 24 (2), 105–111 (in Chinese with English abstract).

Ji, X.X., Zhou, S., Chen, Q., Liu, D.M., Li, D.W., 2016. Provenance and tectonic setting of the Kunyang Group in central Yunnan Province. Geol. China 43 (3), 857–878 (in Chinese with English abstract).

Jin, Z.G., et al., 2016. Ore genesis of the Nayongzhi Pb-Zn deposit, Puding City, Guizhou Province, China: Evidences from S and in situ Pb isotopes. Acta Petrol. Sin. 32 (11), 3441–3455.

Koppel, V., Schroll, E., 1988. Pb-Isotope evidence for the origin of lead in strata-bound Pb-Zn deposits in triassic carbonates of the eastern and southern alps. Miner. Deposita 23 (2), 96–103.

Leach, D.L., Sangster, D.F., 1993. Mississippi Valley-type lead-zinc deposits. Miner. Deposit Model. 289–314.

Leach, D.L. et al., 2005. Sediment-hosted lead-zinc deposits: a global perspective. Economic Geology 100th anniversary volume: 561–607.

Leach, D.L., et al., 2010a. Sediment-hosted lead-zinc deposits in earth history. Econ. Geol. 105 (3), 593–625.

Leach, D.L., Taylor, R.D., Fey, D.L., Diehl, S.E., Saltus, R.W., 2010b. A deposit model for Mississippi Valley-Type lead-Zinc ores, U.S. Geological Survey Science Investigation Report 2010–5070A.

Li, X.J., Wu, H.D., Duan, J.S., 1984. The stratigraphic seqence of the Kunyang Group and its top and bottom boundaries. Geol. Rev. 30 (5), 399–408 (in Chinese with English abstract).

Li, L.J., Liu, H.T., Liu, J.S., 1999. A discussion on the source bed of Pb-Zn-Ag deposits in Northeast Yunnan. Geol. Explor. Nonferrous Met. 8 (6), 333–339 (in Chinese with English abstract).

Li, W.B., et al., 2002a. Sources of ore-forming materials in Huize suuperlarge zinc-lead deposit, Yunnan Province. Evidence from contents of ore-forming element in strata

and basalts from margin of ore district. Miner. Deposits 21 (Supp.), 413–416 (in Chinese).

Li, X.H., Li, Z.X., Zhou, H.W., Liu, Y., Kinny, P.D., 2002b. U-Pb zircon geochronology, geochemistry and Nd isotopic study of Neoproterozoic bimodal volcanic rocks in the Kangdian Rift of South China: implications for the initial rifting of Rodinia. Precambrian Res. 113 (1–2), 135–154.

Li, W.B., Huang, Z.L., Zhang, G., 2006. Sources of the ore metals of the Huize ore field in Yunnan province: constraints from Pb, S, C, H, O and Sr isotope geochemistry. Acta Petrol. Sin. 22 (10), 2567–2580.

Li, W.B., Huang, Z.L., Yin, M.D., 2007. Isotope geochemistry of the Huize Zn-Pb ore field, Yunnan Province, Southwestern China: Implication for the sources of ore fluid and metals. Geochem. J. 41 (1), 65–81.

Li, H.K., Zhang, C.L., Yao, C.Y., Xiang, Z.Q., 2013. U-Pb zircon age and Hf isotope compositions of Mesoproterozoic sedimentary strata on the western margin of the Yangtze massif. Sci. China Earth Sci. 56 (4), 628–639.

Li, B., et al., 2015. Geological, rare earth elemental and isotopic constraints on the origin of the Banbanqiao Zn-Pb deposit, southwest China. J. Asian Earth Sci. 111, 100–112.

Liu, H.C., 1995. Emeishan basalt and Pb-Zn metallogenesis. Geol. Explor. 31 (4), 1–6 (in Chinese with English abstract).

Liu, H.C., Lin, W.D., 1999. Metallogeny of Pb–Zn–Ag Ore Deposits in Northeast Yunnan, China. Yunnan University Press, China.

Liu, Y.P., Li, C.Y., Gu, T., Wang, J.L., 2000. Isotopic constraints on the source of ore-forming materials of Dulong Sn-Zn polymetallic deposit, Yunnan. Geol. Geochem. 28 (4), 75–82 (in Chinese with English abstract).

Luczaj, J.A., Millen, T., Martin, J., 2007. A lead-isotopic study of Galena from Eastern Wisconsin: Evidence for lead sources in Precambrian basement rocks, Geological Society of America, North-Central/South Central Meeting, Lawrence Kansas, pp. 67.

Luo, D.F., Huang, Z.L., Wang, F., Zhou, J.X., Li, X.B., 2012. Mechanism of transportation and precipitation of mineralization elements in the Huize super-large Pb-Zn deposit, Yunnan Province, China. Acta Mineral. Sin. 32 (2), 288–293 (in Chinese with English abstract).

Lv, S.K., Dai, H.G., 2001. A review of the set-up of Kunyang Group's sequence and the discovery of important ore-bearing horizons in Kang-Dian area. Yunnan Geol. 20 (1), 1–24 (in Chinese with English abstract).

Macfarlane, A.W., Petersen, U., 1990. Pb isotopes of the hualgayoc area, northern peru – Implications for metal provenance and genesis of a cordilleran-polymetallic-mining-district. Econ. Geol. Bull. Soc. Econ. Geol. 85 (7), 1303–1327.

Meng, G.H., 2014. An analysis of the geological feature and metallogenesis of Huize Pb-Zn deposit. Yunnan Geol. 33 (3), 380–383 (in Chinese with English abstract).

Pang, W.H., Ren, G.M., Sun, Z.M., Yin, F.G., 2015. Division and correlation of Paleo-Mesoproterozoic strata on the western margin of Yangtze block: Evidence from the U-Pb age of tuff zircon in the Tongan Formation. Geol. China 42 (4), 921–936 (in Chinese with English abstract).

Pedersen, M., 2000. Lead isotope signatures of sedimentary rocks as a tool for tracing ore lead sources: a study of base-metal and barite occurrences in Jameson Land Basin, central East Greenland. Trans. Inst. Min. Metall., Sect. B 109, B49–B59.

Portra, A., Moyers, A., 2017. Constraints on the sources of ore metals in Mississippi Valley-type deposits in central and east Tennessee, USA, using Pb isotopes. Ore Geol. Rev. 81 (Part 1), 201–210.

Reuter, J.H., Perdue, E.M., 1977. Importance of heavy metal-organic matter interactions in natural-waters. Geochim. Cosmochim. Acta 41 (2), 325–334.

Schneider, J., Boni, M., Lapponi, F., Bechstadt, T., 2002. Carbonate-hosted zinc-lead deposits in the Lower Cambrian of Hunan, South China: A radiogenic (Pb, Sr) isotope study. Econ. Geol. Bull. Soc. Econ. Geol. 97 (8), 1815–1827.

Shellnutt, J.G., Wang, K.L., 2014. An ultramafic primary magma for a low Si, high Ti-Fe gabbro in the Panxi region of the Emeishan large igneous province, SW China. J. Asian Earth Sci. 79, 329–344.

Shellnutt, J.G., Zhou, M.F., Yan, D.P., Wang, Y.B., 2008. Longevity of the Permian Emeishan mantle plume (SW China): 1 ma, 8 Ma or 18 Ma? Geol. Mag. 145 (3), 373–388.

Shelton, K.L., et al., 1995. Sulfur Isotope Evidence for Penetration of Mvt Fluids into Igneous Basement Rocks, Southeast Missouri, USA. Miner. Deposita 30 (5), 339–350.

Slobodnik, M., Jacher-Sliwczynska, K., Taylor, M.C., Schneider, J., Dolnicek, Z., 2008. Plumbotectonic aspects of polymetallic vein mineralization in Paleozoic sediments and Proterozoic basement of Moravia (Czech Republic). Int. J. Earth Sci. 97 (1), 1–18.

Sun, Z.M., et al., 2009. SHRIMP U-Pb dating and its stratigraphic significance of tuff zircons from Heishan Formation of Kunyang Group, Dongchuan area, Yunnan Province, China. Geol. Bull. China 28 (7), 896–900 (in Chinese with English abstract).

Sverjensky, D.A., 1981. The origin of a Mississippi valley-type deposit in the viburnum-trend, Southeast Missouri. Econ. Geol. 76 (7), 1848–1872.

Vaasjoki, M., Gulson, B.L., 1986. Carbonate-hosted base-metal deposits – Lead isotope data bearing on their genesis and exploration. Econ. Geol. 81 (1), 156–172.

Wilkinson, J.J., 2014. Sediment-hosted zinc-lead mineralization: Processes and perspectives. In: Turekian, K., Holland, H. (Eds.), Treatise on Geochemistry, second ed. Elsevier, Oxford, pp. 219–249.

Wu, Y., Zhang, C.Q., Mao, J.W., Ouyang, H.G., Sun, J., 2013. The genetic relationship between hydrocarbon systems and Mississippi Valley-type Zn-Pb deposits along the SW margin of Sichuan Basin, China. Int. Geol. Rev. 55 (8), 941–957.

Yan, D.P., Zhou, M.F., Song, H.L., Fu, Z.R., 2003. Structural style and tectonic significance of the Jianglang dome in the eastern margin of the Tibetan Plateau, China. J. Struct. Geol. 25 (5), 765–779.

Yuan, H.L., et al., 2015. High precision in-situ Pb isotopic analysis of sulfide minerals by femtosecond laser ablation multi-collector inductively coupled plasma mass spectrometry. Sci. China Earth Sci. 58 (10), 1713–1721.

Zartman, R.E., Haines, S.M., 1988. The Plumbotectonic Model for Pb Isotopic Systematics among Major Terrestrial Reservoirs – a Case for Bi-Directional Transport. Geochim.

Cosmochim. Acta 52 (6), 1327–1339.

Zhang, P.P., 2009. A comparison of geochemistry of microelement characters among superlarge Pb-Zn deposit in Kangdain area. Hunan Nonferrous Metals 25 (2), 4–7 (in Chinese with English abstract).

Zhang, C.Q., et al., 2005. Distribution, characteristics and genesis of Mississippi Valley-type lead-zinc deposits in Sichuan-Yunnan-Guizhou area. Miner. Deposits 24 (3), 336–348 (in Chinese with English abstract).

Zhang, C.Q., Wu, Y., Hou, L., Mao, J.W., 2015. Geodynamic setting of mineralization of Mississippi Valley-type deposits in world-class Sichuan-Yunnan-Guizhou Zn-Pb triangle, southwest China: Implications from age-dating studies in the past decade and the Sm-Nd age of Jinshachang deposit. J. Asian Earth Sci. 103, 103–114.

Zhao, X.F., et al., 2010. Late Paleoproterozoic to early Mesoproterozoic Dongchuan Group in Yunnan, SW China: Implications for tectonic evolution of the Yangtze Block. Precambrian Res. 182 (1–2), 57–69.

Zhong, K.H., Liao, W., Song, M.Y., Zhang, Y.Q., 2013. Discussion on sulfur isotope of Huize Pb-Zn deposit in Yunnan, China. J. Chengdu Univ. Technol. 40 (2), 130–138

(in Chinese with English abstract).

Zhong, Y.T., He, B., Mundil, R., Xu, Y.G., 2014. CA-TIMS zircon U-Pb dating of felsic ignimbrite from the Binchuan section: Implications for the termination age of Emeishan large igneous province. Lithos 204, 14–19.

Zhou, C.X., Wei, C.S., Li, C.Y., 1998. Lower Sinian igneous rock suits along the southwestern Yangtze Block. Acta Mineral. Sin. 18 (4), 401–410 (in Chinese with English abstract).

Zhou, C.X., Wei, C.S., Guo, J.Y., Li, C.Y., 2001. The source of metals in the Qilinchang Zn-Pb deposit, northeastern Yunnan, China: Pb-Sr isotope constraints. Econ. Geol. Bull. Soc. Econ. Geol. 96 (3), 583–598.

Zhou, J.X., Huang, Z.L., Yan, Z.F., 2013a. The origin of the Maozu carbonate-hosted Pb-Zn deposit, southwest China: Constrained by C-O-S-Pb isotopic compositions and Sm-Nd isotopic age. J. Asian Earth Sci. 73, 39–47.

Zhou, J.X., Huang, Z.L., Zhou, M.F., Li, X.B., Jin, Z.G., 2013b. Constraints of C-O-S-Pb isotope compositions and Rb-Sr isotopic age on the origin of the Tianqiao carbonate-hosted Pb-Zn deposit, SW China. Ore Geol. Rev. 53, 77–92.